



Full Paper

APPLICATION OF ROOFTOP FUNCTIONS IN THE ANALYSIS OF ANTENNA SYSTEMS

E. Obayiuwana

Department of Electrical and Electronic Engineering,
Obafemi Awolowo University, Ile-Ife, Nigeria
obayiuwanaenoruwa@oauife.edu.ng

S.A. Adeniran

Department of Electrical and Electronic Engineering,
Obafemi Awolowo University, Ile-Ife, Nigeria

ABSTRACT

In this paper, we report the analyses of a single element antenna and array antenna using rooftop function as a basis and testing functions to model the current distribution on the antennas. The Method of Moments (MoM) was used to obtain matrix equation from the Electric Field Integral Equation (EFIE) from which the solution to the current distribution was obtained and validate using the Numerical Electromagnetic Code (NEC) software. The input impedance for dipole antenna was obtained and compared against measured results and other electromagnetic computational technique for a dipole antenna. A minimum convergence error percent of 0.03% was observed at the use of 30 rooftop functions. The single element wire antenna input impedance obtained produced better result and converged faster than the use of pulse testing technique. The antenna array characteristics simulated using the results obtained from a single dipole element, achieved the end-fire, broad-side and electronic beam steering (scanning) characteristics of linear array antenna.

Keywords: Method of Moment, Rooftop Function, Antenna Systems Analysis, Computational Electromagnetics.

1. INTRODUCTION

The earliest known rigorous approach to the analysis of wire antenna was by Pocklington in 1897. The integral equation he formulated was named after him. This Integral equation is an integro-differential type of the Electric Field Integral Equation (EFIE), with unknown current distribution along the cylindrical wire. It could not be solved numerically, such that for a long time its value was purely academic.

A different integral equation for modelling thin wire structures was put forward in 1938 (Hallen, 1938). This was derived from EFIE for thin cylindrical wires. Nomura and Hatta (1952) and Storm (1953) proposed the method of moment for the analysis of cylindrical antenna by means of the Hallen's Equation, the solution was very restricted, because the classical computational means available then were not suitable for numerical solution of integral equations. The Pocklington analysis is difficult to implement but gives a more accurate result compared to Hallen analysis for wire antenna.

The first numerical solution of wire-structure antenna was due to (Richmond, 1965). He applied the sub-domain rectangular basis function and entire-domain basis function to solve the Pocklington equation for cylindrical wire structures using the point matching

procedure. Harrington, in his classical work in 1967, introduced the method of moment (MoM) for solving electromagnetic-field problems in general and the thin wire-antenna problem in particular. In tackling the wire antenna problems, he used both the point matching and Galerkin procedures for the first time to obtain its solutions (Harrington, 1967). Many of the works which followed thereafter were based on the MoM.

Most antenna problems are usually modelled using EFIE, which are derived from the Maxwell Equations (Wandzura et al., 1992). Various numerical /computer algorithms have been developed to solve the EFIE for various practical antennas. The most accurate algorithm for solving the EFIE is the MoM but this is usually complex and difficult to implement. The computational accuracy of results obtained, using Method of Moment are largely affected by the choice of basis functions in the modelling of the current distribution on the antenna system (Kolundzija et al., 1998), (Canning, 1993).

Therefore, it is important to look for an optimum basis function that will produce a fast converging result, easy to implement and that will give accurate results. The Numerical Electromagnetic Code (NEC) is the most powerful commercial code and was introduced by (Burke and Paggio, 1981). In this work, rooftop function is used as the basis function and testing function to model the unknown current distribution on the antenna. The result obtained is compared with the results obtained using NEC. The modelled current distribution on the antenna is then used to determine the input impedance, radiation pattern of single element wire antenna and to predict the beam scanning characteristics of the phase array. The input impedance results for single element are compared against experimental measurements and results obtained using other electromagnetic computational techniques

2. THE ELECTRIC FIELD INTEGRAL EQUATION

An antenna carrying current density $\vec{J}(\vec{r})$ has a radiated electric field given as

$$\nabla^2 \vec{E}(\vec{r}) + k^2 \vec{E}(\vec{r}) = j\omega\mu \vec{J}(\vec{r}) - \frac{1}{j\omega\epsilon} \nabla(\nabla \cdot \vec{J}(\vec{r}')) \quad (1)$$

where $\vec{E}(\vec{r})$ is the radiated E-field, k is the wave number and

$\vec{J}(\vec{r}')$ is the source current density. Maxwell's equations are linear,

hence we consider $\vec{J}(\vec{r}')$ as a superposition of point sources distributed over some volume. Therefore, if we know the response of a point source or the Green's function of a point source we can solve the original problem by integrating this response over the volume. This idea is made use of to convert (1) into an Electric field integral equation

$$\vec{E}(\vec{r}) = -j\omega\mu \iiint_{V'} \vec{G}(\vec{r}, \vec{r}') \left(\vec{J}(\vec{r}') + \frac{1}{k^2} \nabla' \nabla' \cdot \vec{J}(\vec{r}') \right) dV' \quad (2)$$

where $\vec{G}(\vec{r}, \vec{r}')$ is the Green's function, \vec{r} is the field observation point, \vec{r}' is current source point and

$$\vec{G}(\vec{r}, \vec{r}') = \frac{e^{-jk|\vec{r}-\vec{r}'|}}{4\pi|\vec{r}-\vec{r}'|} \quad (3)$$

However, in many cases of practical interest, it may be difficult or impossible to directly solve this equation for the fields. A remedy, an auxiliary vector potential that can be used to solve for the radiated fields needs to be derived. The vector potential is obtained via integral equation of the currents, and the radiated fields are obtained directly from the vector potential. Vector potential formulation is used extensively in the analysis of antenna radiation and scattering problems, and used frequently in this work. The radiated E-field in

terms of auxiliary vector potential $\vec{A}(\vec{r})$ is given by

$$\vec{E}(\vec{r}) = -j\omega\vec{A}(\vec{r}) - \frac{j}{\omega\mu\epsilon} \nabla(\nabla \cdot \vec{A}(\vec{r})) \quad (4)$$

where

$$\vec{A}(\vec{r}) = \mu \iiint_{V'} \vec{J}(\vec{r}') \frac{e^{-jk|\vec{r}-\vec{r}'|}}{4\pi|\vec{r}-\vec{r}'|} dV' \quad (5)$$

2.1. Far Fields

When the observation point is located very far away from the source, $k\vec{r} \gg 1$, approximations can be made that greatly simplify the computation of the radiated field. In this case \vec{r} and $\vec{r}-\vec{r}'$

are virtually parallel. Under this assumption, \vec{r} can reasonably be approximated as,

$$\vec{r} = \begin{cases} r, & \text{for amplitude variations} \\ r - \vec{r}' \cdot \hat{r}, & \text{for phase variations} \end{cases} \quad (6)$$

It has been shown that the far-field component becomes a proportional to $\frac{1}{r}$ (Morita *et al*, 1990). The far electric field will therefore be computed as

$$\begin{aligned} \vec{E}(\vec{r}) &= -j\omega\vec{A}(\vec{r}) \\ &= -\frac{j\omega\mu}{4\pi r} \iiint_{V'} \vec{J}(\vec{r}') e^{-jk(r-\vec{r}' \cdot \hat{r})} dV' \end{aligned} \quad (7)$$

(8a)

$$= -\frac{j\omega\mu e^{-jk r}}{4\pi r} \iiint_{V'} \vec{J}(\vec{r}') e^{jk \vec{r}' \cdot \hat{r}} dV' \quad (8b)$$

3. MODELLING TECHNIQUE

For most problems of practical interest, the derived Integral Equation cannot be solved analytically, hence the application of computational methods to obtain the solution. The MoM is a technique used to convert the integral equation into a linear system that can be solved numerically using a digital computer.

The Rooftop function is used as the basis function to model the expected behaviour of the unknown current throughout the problem domain. A rooftop function is defined as

$$f_n(x) = \begin{cases} \frac{x-x_{n-1}}{x_n-x_{n-1}}, & x_{n-1} \leq x \leq x_n \\ \frac{x_{n+1}-x}{x_{n+1}-x_n}, & x_n \leq x \leq x_{n+1} \end{cases} \quad (9)$$

An inner product or moment between a basis function $f_n(\vec{r}')$ and a testing function $f_m(\vec{r})$ is defined as

$$\langle f_m, f_n \rangle = \int_{f_m} \vec{f}_m(\vec{r}) \cdot \int_{f_n} \vec{f}_n(\vec{r}') d\vec{r}' d\vec{r} \quad (10)$$

Requiring the inner product of each testing function with the residual function to be zero yields,

$$\sum_{n=1}^N a_n \langle f_m, L(f_n) \rangle = \langle f_m, g \rangle \quad (11)$$

which produces a $N \times N$ matrix equation given by

$$[Z_{mn}][a_n] = [b_m], \quad (12)$$

with matrix elements

$$z_{mn} = \langle f_m, L(f_n) \rangle \quad (13)$$

and right-hand side vector elements

$$b_m = \langle f_m, g \rangle \quad (14)$$

where $L(\bullet)$, g operator and forcing are function, respectively.

In the MoM, each Rooftop function interacts with all others by means of the Green's function

3.1. Thin Wire Approximation

Consider the dipole antenna shown in Figure 1 to be a perfectly conducting thin wire with the length, $L = 1$ m and radius, $a = 5$ mm operating at a wavelength of 1m and (i.e. $a \ll \lambda$ and $L \gg a$

), oriented in \hat{z} -direction. An incident electric field $\vec{E}^i(\vec{r})$ excites

on this wire a surface current $\vec{J}(\vec{r}')$. Since the wire is very thin, and

assuming that $\vec{J}(\vec{r}')$ can be written in terms of a \hat{z} -oriented

filamentary current $I_z(\vec{r}')$ as



$$\vec{J}(\vec{r}') = \frac{I_z(z')}{2\pi a} \hat{z} \quad (15)$$

In cylindrical coordinates, the corresponding magnetic vector potential A_z in terms of the surface integral is written as

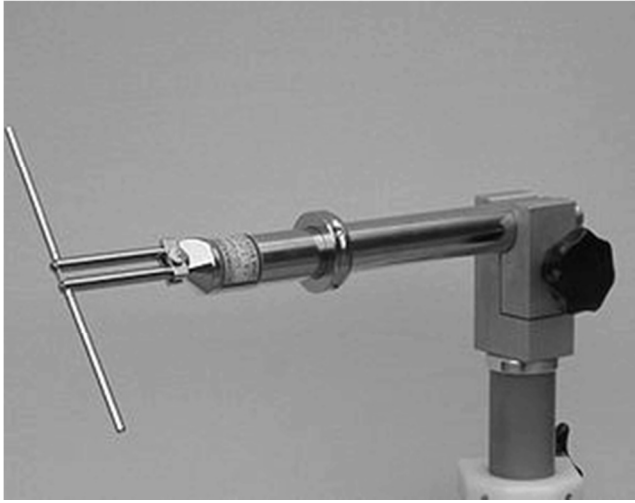


Figure 1: Single Dipole Antenna

$$A_z(\rho, \phi, z) = \mu \int_{-\frac{L}{2}}^{\frac{L}{2}} \int_0^{2\pi} \frac{I_z(z')}{2\pi} \frac{e^{-jk r}}{4\pi r} d\phi' dz' \quad (17)$$

noting that $\rho' = a$, and that the source point is at the surface of the thin wire conductor, where a is the radius of the conductor. Therefore,

$$r = \sqrt{(z-z')^2 + \rho^2 + a^2 - 2a\rho\cos(\phi-\phi')} \quad (17a)$$

If a is assumed to be very small, r can be approximated as

$$r = \sqrt{(z-z')^2 + \rho^2} \quad (17b)$$

hence,

$$A_z(\rho, z) = \mu \int_{-\frac{L}{2}}^{\frac{L}{2}} I_z(z') \frac{e^{-jk r}}{4\pi r} dz' \quad (18)$$

The radiated field obtained from (4) is

$$E_z^s = -j\omega A_z - \frac{j}{\omega\mu\epsilon} \frac{\partial^2}{\partial z^2} A_z, \quad (19)$$

by enforcing the boundary condition of zero tangential electric field on the surface of the wire,

$$E_z^s = -E_z^i \quad (20)$$

The thin wire EFIE in terms of the incident field E_z^i is

$$E_z^i(z) = \frac{j}{\omega\epsilon} \int_{-L/2}^{L/2} I_z(z') \left[\frac{\partial^2}{\partial z^2} + k^2 \right] \frac{e^{-jk r}}{4\pi r} dz' \quad (21)$$

Equation (21) is called Pocklington's integral equation (Sadiku, 2001).

3.2. Source Excitation Modelling

The excitation source for the dipole antenna is modelled by a delta-gap source. The delta-gap source treats the feed as if the electric

field impressed by the feed line exists only in the gap between the antenna terminals and is zero outside, that is, no fringing in the region of the feed, the current is of course displacement current, rather than conduction current; it is effectively the former which the MoM is approximating in the feed region, but it still needs a segment (even though it is fictitious) and its associated expansion function in order to do this (Davidson, 2005). The delta-gap source model assumes that the impressed electric field in the thin gap between the antenna terminals can be expressed as

$$\vec{E}_z^i = \frac{V_o}{\Delta_z} \hat{z}, \quad (22)$$

where Δ_z is the width of the gap, and V_o is usually set to unity. In the numerical simulation, this field exists inside one wire segment and is zero outside (Gibson, 2008). The resulting excitation vector will have nonzero elements only for basis functions defined within that segment.

3.2. Linear Array antenna

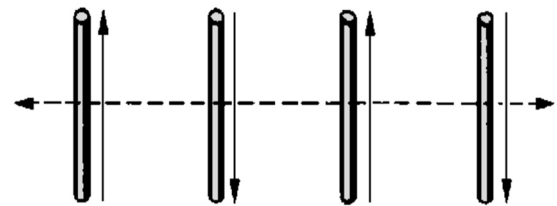
A single element antenna is usually not enough to achieve some required technical specifications. That happens because its performances are limited. Usually the radiation pattern of a single element is relatively wide, and each provides low values of directivity (gain). When an antenna array has elements arranged in a straight line, it is referred to as a linear array. A uniform array consists of equi-spaced elements, which are fed with current of equal magnitude and can have progressive phase-shift along the array. Figure 2 shows a uniform linear array of N elements equally spaced at distance d apart with identical amplitude excitation and has a progressive phase difference of β between the successive elements.

The radiated electric field of the linear array equals the product of the radiated electric field of single element antenna at the reference point and the array factor. The array factor (AF) is given by

$$AF = \sum_{n=1}^N e^{j(n-1)(kd \cos \theta + \beta)}, \quad (23)$$

where k the wave number, d is the element spacing, β is the phase shift and θ is the angle of radiation.

The linear array antenna is analysed using the radiated field from a single dipole antenna that serves as the reference element with the linear array factor (AF).



A. TOP VIEW OF ARRAY

B. SIDE VIEW OF ARRAY

Figure 2: Linear Array (with N-elements)

4. RESULTS AND DISCUSSIONS

From equation (21), numerical computations for the input impedance matrix, which are generally complex Toeplitz Matrix, from which the current distribution, input impedance, and far field

radiation pattern are gotten for a radiating dipole antenna of signal frequency 300MHz, radiating in a free-space, are computed using 36, 48 and 60 unknown basis rooftop functions. The current distribution results obtained for wire dipole analysis are shown in figure 3. The current distribution plots showed that the magnitude of current values at both ends of the dipole antenna decays to zero. This result supports the electromagnetics boundary conditions that exist between the antenna and dielectric air medium. The current distribution obtained showed that the position of current anti-node is located at the mid-section of the dipole antenna, which is practically the feed or excitation point. This distribution showed that current nodes exit at the tips or ends of the dipole antenna of length $\lambda/2$ with the current Anti-node at its mid-section. Figure 4 shows that the current distribution result obtained compares well with that obtained using the NEC.

The Figure 5 and 6 compared the input impedance obtained in this work to that of experimental measurement of $72.0 + j0$ Ohms at resonance. The input impedance converges to the experimental value. The input impedance value for the dipole antenna improves as the number of roof top basis functions increases and the input impedance value converged approximately to $72.2 + j1.3$ Ohms. The computed convergence percentage error is 0.4% .

It is observed in this work that the real part of the input impedance converges better than the reactive part to the experimental value.

Figure 7 and 8 compared the input resistance and input reactance obtained in this work to that of reported by Eric D. Caswell against the number of basis function used. Figures 7 and 8 showed that the input impedance obtained from this work converges faster than that obtained using sinusoidal basis functions and testing functions. The input impedance convergence result of $77 + j5$ ohms was reported by Eric D. Caswell (Caswell, 1998), using sinusoidal basis functions and testing functions. A perfect resonant single dipole antenna has an input Impedance of experimental measurement value of $72.0 + j0$ Ohms. This work shows improved results using rooftop basis functions and testing functions as compared to the use of sinusoidal basis functions and pulse testing functions. Figure 9 showed the input resistance percent error convergence result. The result showed a minimum convergence error of approximately 0.03% , at the use of 30 rooftop functions. The percent error

convergence P_e is computed using the formula

$$P_e = \frac{O_v - T_v}{T_v} \times 100 \% \quad (24)$$

where O_v is the obtained value and T_v is the true value.

The far-field result obtained for a single element dipole antenna of length 0.5λ is presented in figure 10. The radiation pattern results for eight-element (N=8) linear arrays are presented in figures 11 and 12. Figures 11 and 12 show the results obtained for End-fire and Broadside configurations using eight single element dipole antennas, with inter-element spacing (d) and phase shift (β) of 0.25λ , -90° , 0.5λ and 0° , respectively. The results for phase/ (scanning) array through arbitrary desired angle of radiation (θ_0) of 80° , 60° and 50° are presented in Figure 13, 14 and 15 respectively.

5. CONCLUSIONS

The EFIE equation for the analysis of wire antenna was implemented using MATLAB codes. The current distributions along the dipole antenna using rooftop functions compared well with NEC.

The input impedance for dipole wire antenna obtained using rooftop functions as basis and test functions are more accurate and converged faster than the results obtained using sinusoidal basis

functions and testing functions. The input impedance value for the dipole antenna improves as the number of roof top basis functions increases and the input impedance value converged approximately to $72.2 + j1.3$ Ohms. The computed convergence percentage error is 0.4% .

Far-Electric field (E-field) agrees with the E-field radiation pattern of a practical dipole antenna. The result obtained from single element dipole antenna, when applied to linear array dipole antenna, produced good results.

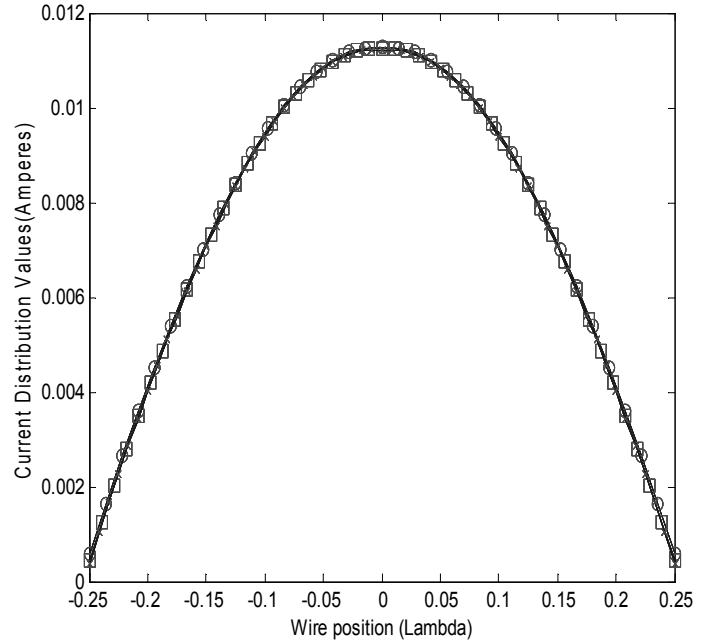


Figure 3: Current distributions over wire length of 0.5λ , using 36(\circ), 48(\square) and 60(\times) rooftop basis Functions

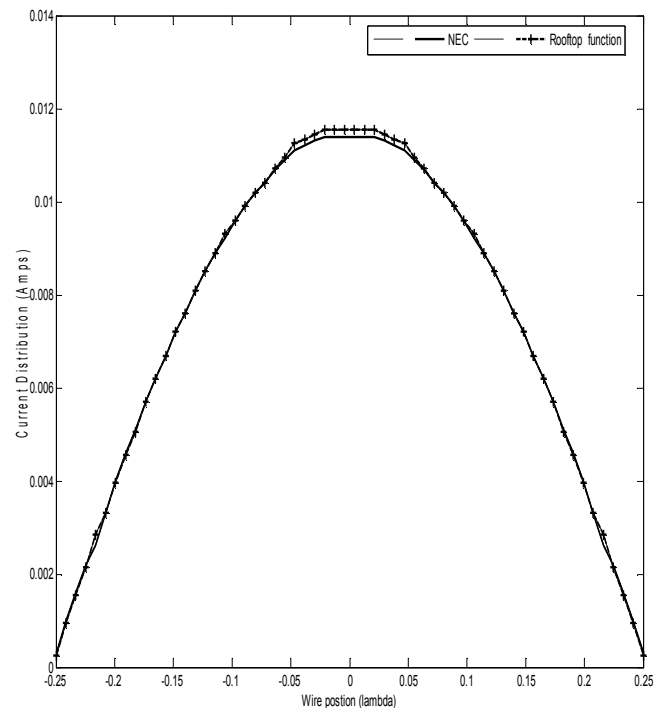


Figure 4: Comparison of results from rooftop function and NEC for Current distribution for dipole wire antenna operating at 300MHz

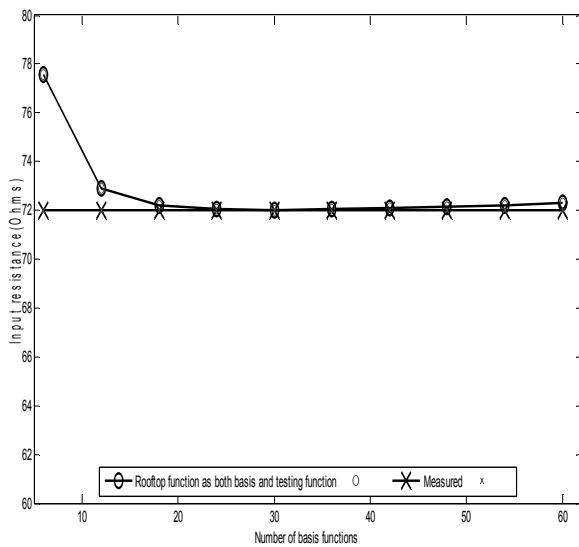


Figure 5: Comparison of results from rooftop function and experimental results for an input resistance of a dipole antenna at resonance

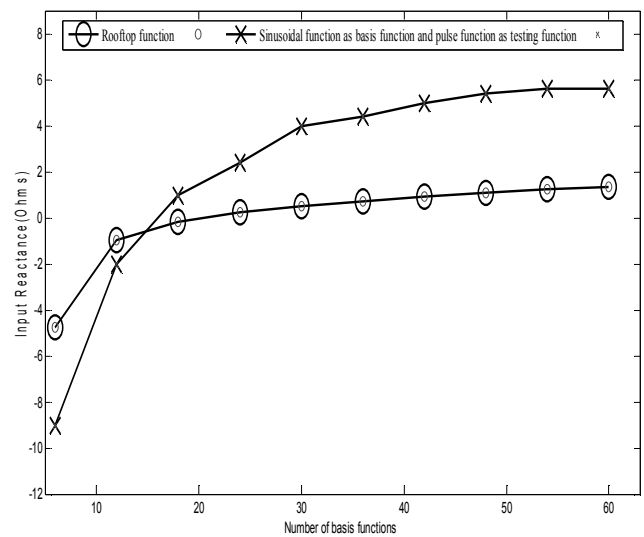


Figure 8: Comparison of results from rooftop function and sinusoidal function analysis for input reactance of a dipole antenna at 300Hz

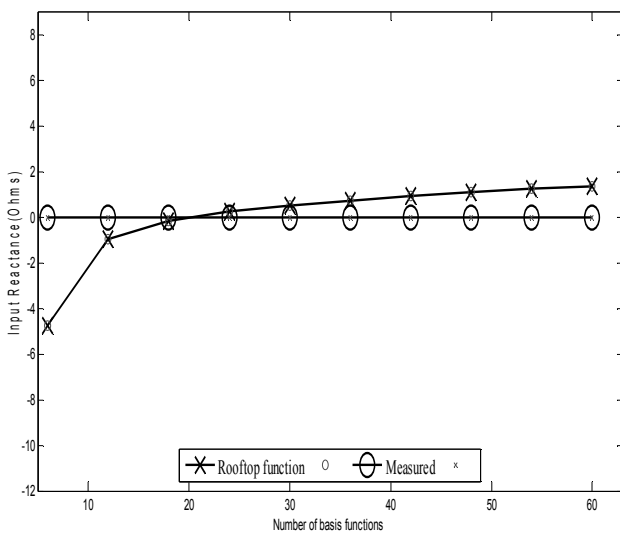


Figure 6: Comparison of results from rooftop function and experimental results for an input reactance of a dipole antenna at resonance

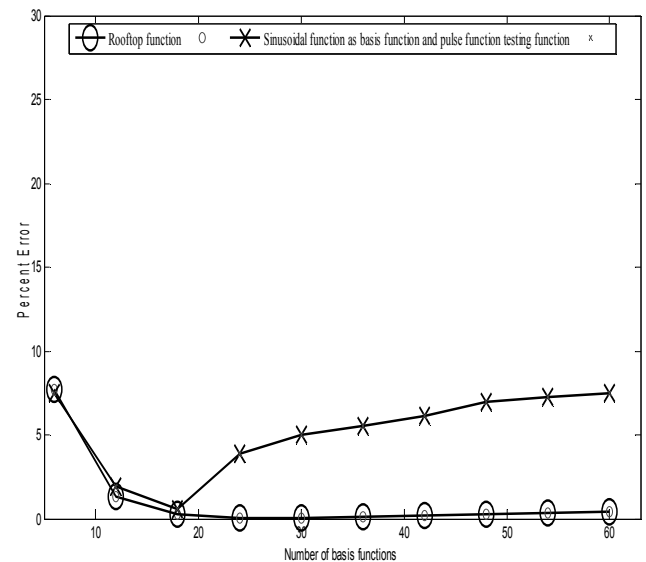


Figure 9: Comparison of input resistance percent error results for rooftop function and sinusoidal function for a dipole antenna at 300MHz

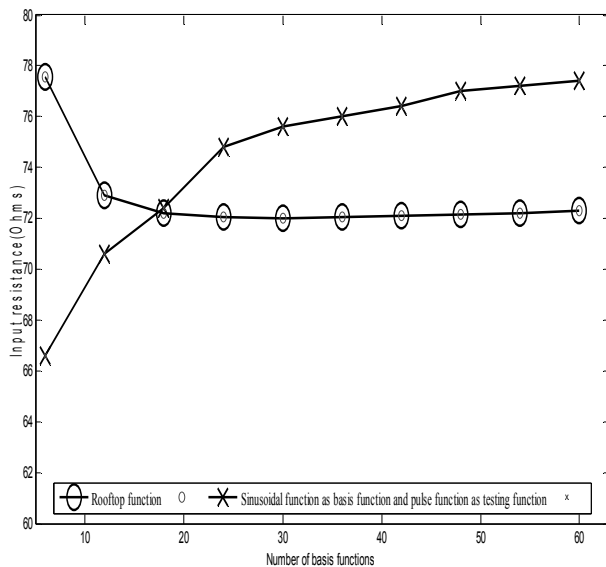


Figure 7: Comparison of results from rooftop function and sinusoidal function analysis for input resistance of a dipole antenna at 300Hz

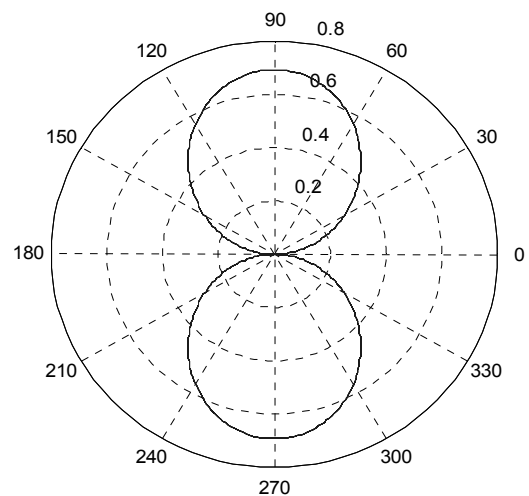
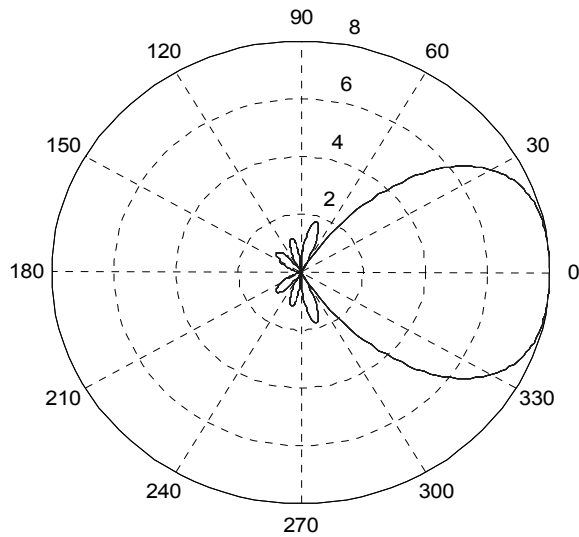
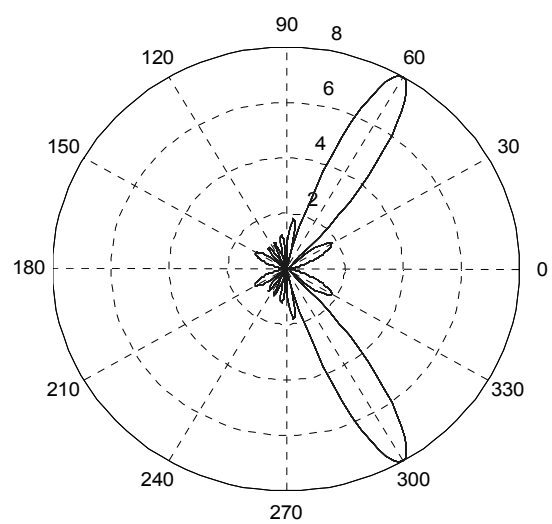
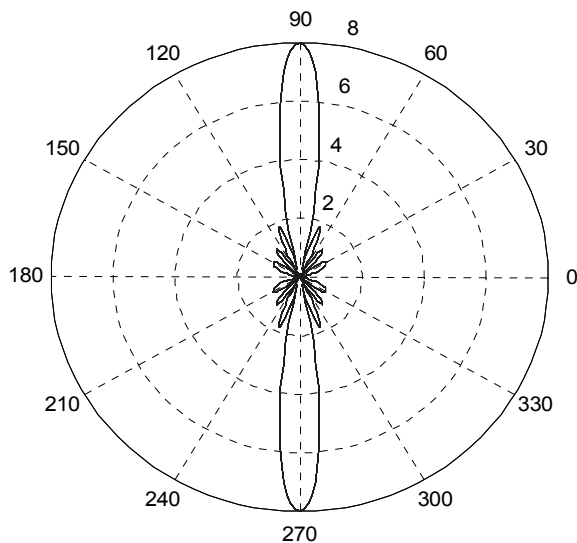
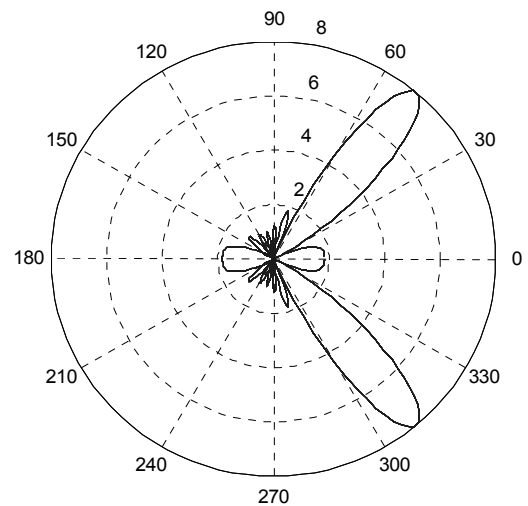
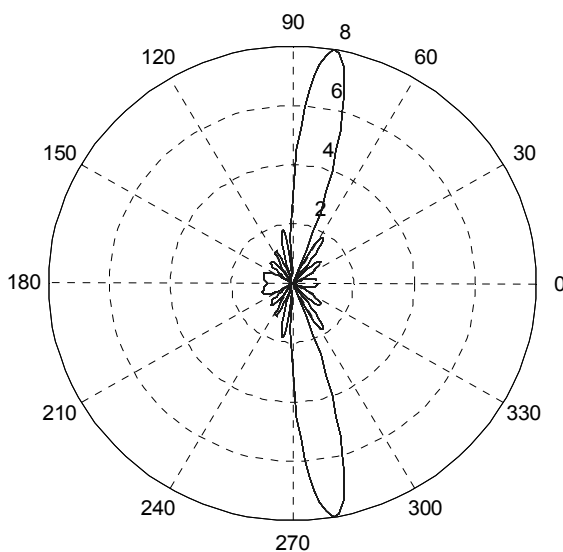


Figure 10: Far-Field radiation Pattern for single dipole wire antenna of length 0.5λ , using 60 rooftop basis functions


Figure 11: Radiation pattern for End-fire linear array with $N = 8, d = 0.25\lambda, b = -90^\circ$

Figure 14: Polar plot result for Phase array with $N=8, d=0.5\lambda$ and $\theta_0 = 60^\circ$

Figure 12: Radiation Pattern for Broadside linear array with $N = 8, d = 0.5\lambda, b = 0^\circ$

Figure 15: Polar plot result for Phase array with $N=8, d = 0.5\lambda$ and $\theta_0 = 50^\circ$

Figure 13: Polar plot result for Phase array with $N=8, d = 0.5\lambda$ and $\theta_0 = 80^\circ$

REFERENCES

- Canning, F. X., Improved impedance matrix localization method [EM problems], *IEEE Trans. Antenna Propagation*, 1993, 41, pp 659–667.
- Caswell, E.D., Analysis of a Helix Antenna Using a Moment Method Approach with Curve Basis and Testing Functions, Virginia Polytechnic Institute and State University, U.S.A.
- David, B. D., *Computational Electromagnetic and Microwave Engineering* (Department of Electrical and Electronic, University of Stellenbosch, South Africa, 2005)
- G. Burke and A. Poggio, Numerical Electromagnetics Code (NEC)-Method of Moments, Part 2: Program Description—Code, 1981
- Gibson C. Walton, *Method of Moments in Electromagnetics* (Chapman & Hall/CRC Taylor & Francis Group New York, 2008)
- Hallen, E. (1938) "Theoretical investigations into the transmitting and receiving qualities of antennae," *Nova Acta (Uppsala)*, vol. II, 1–44, 1938.
- Harrington, R. F., *Field Computation by Moment Methods* (Macmillan, New York, 1968)
- Kolundzija, B.M. and Sarkar, T.K., On the choice of optimal basis functions for MoM/SIE, MoM/VIE, FEM and hybrid methods, *IEEE Trans. Antenna Propagation*, 1998, 278 – 281 vol.1
- Morita, N., Kumagai, N. and Mautz, J.R., *Integral Equation Methods for Electromagnetics* (Artech House, Boston, 1990)
- Nomura, Y. and Hatta, T., the theory of a linear Antenna 1, *Technical report*, Tohoku University, Vol.17, Part 1, 1952



- Pocklington, H. C., Electrical oscillations in wire, *Camb. Phil. Soc. Proc.* 9, 1990, 24- 332.
- Richmond, J. H., Digital solutions of the rigorous equations for scattering problems *Proc. IEEE* 53, 1965, pp. 796-804.
- Sadiku, M. N., *Numerical Techniques in Electromagnetics* (second Edition, CRC Press, Boca Raton London, 2001)
- Storm, B., Investigation into Modern Aerial Theory and a new solution of Hallen's Integral Equation for Cylindrical Aerial, Imperial College, London, U.K. 1953.
- Wandzura S.M. Thorington, C.B. Turley, C.B. Turley, R.S. and Hamilton, L.R. Fast Fourier transform techniques for solving the electric field integral Equation for a periodic body *Proc. IEEE, Microwave and Antenna propagation.* 1992, pp 401-406, Vol.139.